ORIGINAL ARTICLE

Breakthrough studies for the sorption of methylene blue dye from wastewater samples using activated carbon derived from waste banana peels

Denga Ramutshatsha-Makhwedzha[1] · Alexis Munyengabe[2] · Mapula Lucey Mavhungu[1] · Richard Mbaya[1] · Jeffrey Baloyi[3]

Abstract

In the current study, an activated carbon derived from waste banana peel using H_2SO_4 was applied for the first time in a packed-bed column for methylene blue (MB) dye removal from wastewater. The pore structure and surface of banana peel activated carbon (BPAC) were investigated using X-ray diffraction, thermogravimetric analysis, scanning electron microscopy, and Brunauer-Emmett-Teller analysis to discover the mechanism of MB sorption. The produced BPAC by H_2SO_4 activation agent has surface area of 361.86 m^2/g and exhibits good thermal stability. The extent of MB breakthrough performance was examined by optimizing flow rate, bed mass, and initial concentration at pH 9. The column's dynamics revealed a strong dependence of breakthrough curves as a function of process conditions. The breakthrough time (t_b), volume of liters processed (L), and adsorption exhaustion rate all increased as bed mass increased but decreased as flow rate and initial concentration increased. Applying linear regression to the experimental data, Yoon-Nelson and Thomas' kinetic model was used to extract column characteristic parameters that could be used in process design. Using environmental water, the waste banana peel activated carbon material demonstrated effectiveness in removing MB to below acceptable levels by processing 1.16 L of water with an initial MB concentration of 40 mg/L using 8 g of sorbent. Nitric acid (3M) was able to regenerate the exhausted bed. Moreover, the sorbent was reused four times with no significant capacity loss. It can be concluded that waste banana peel activated carbon medium is an alternative solution to remediate MB-contaminated wastewater.

Keywords Wastewater · Breakthrough · Methylene blue · Activated carbon · Fixed-bed studies

1 Introduction

Recently, environmental pollution has increased due to mechanization of agricultural fields, industrial revolution, and high technology. Contamination of dyes is considered one of the most dangerous problems threatening human beings as well as aquatic life [1]. The main sources of dyes are industrial wastes such as plastics, leather processing, textiles, rubber, and other industries that use dyes as colorants in their products [2, 3]. Annually, in the textile industry, 1000 tons of dyes are used, in addition to 100 tons expelled into water bodies [1]. These are one of the most dangerous problems facing the scientific community as these dyes remain in flowing water and water bodies for long periods. Therefore, it is important to innovate techniques and methods with high quality and performance to remove these colorants from wastewater. Appropriately, different technologies for the removal of MB have been utilized such as membrane filtration [4], reverse osmosis [5], ozonation [6], chemical precipitation [7], adsorption [8], and electrochemical [9], among others. However, most of these approaches are not economically and qualitatively efficient in removing colorants from industrial effluents. Among them, adsorption has been determined to be an advanced technique due to its simplicity of operation, versatility, low cost, particularly

✉ Denga Ramutshatsha-Makhwedzha
denga.makhwedzha18@gmail.com; makhwedzhad@tut.ac.za

1 Department of Chemical, Metallurgical and Materials Engineering, Tshwane University of Technology, Pretoria West Campus, Private Bag X680, Pretoria, South Africa

2 Department of Chemistry, Tshwane University of Technology, Arcadia Campus, Pretoria 0001, South Africa

3 Smart Places Cluster, Council for Scientific and Industrial Research (CSIR), Pretoria 0001, South Africa

green, and eco-friendly in nature [10–12]. The method has the ability to eliminate small and large organic, toxic, and non-toxic molecules in their solutions without producing hazardous intermediates or fragmenting the molecule [13].

The adsorption technique's efficacy is heavily dependent on analyte properties, adsorbent type, and wastewater matrix composition [14]. Recent studies has concentrated on developing efficient, cost-effective, and environmentally acceptable dye removal adsorbents, as well as optimizing the adsorption process [15–18]. Activated carbon (AC) is the most researched and applied material worldwide in various pollutants removal from wastewater including dyes [19–22]. AC has interesting properties like chemical stability and large specific surface area, which makes it an attractive substrate for the production of various composite materials [23]. Due to its unique structural and chemical properties, AC is considered a universal adsorbent used for removing metal ions from organic compounds and wastewaters. New research results on the use of eco-friendly elements and low-cost bio-adsorbents made from agricultural wastes such as banana peels [24], banana tree [25], peach and apricot kernels [26], olive stones [27], tea waste [28], apple peels [29], corn cobs [30], and coffee grounds [31].

Banana peel is one example of a cost-effective adsorbent. Furthermore, fruit peels and skins contain hemicellulose, cellulose, hydroxyl, pectin molecules, carboxyl, and lignin, which improve adsorbent-adsorbate interactions [32]. Banana peel is a popular sorbent that has been researched by numerous researchers on adsorption of dye [33–36]. Banana peels, as market waste, pose difficulties for environmental disposal. As a result, carbon-rich agricultural leftovers that are dumped could result in greenhouse gas emissions and have a negative impact on the environment. Producing AC from waste materials, particularly agricultural leftovers, would be economically beneficial, would minimize waste and costs, and would produce a low-cost replacement to commercial ACs. Several processes are involved in the synthesis of activated carbon from agricultural waste, including activation, carbonization, and dehydration [37]. Physical and chemical activation are used to produce a wide surface area of activated carbon. Chemical activation is the use of chemicals as an activating agent, such as KOH [38], H_2SO_4 [39], HNO_3 [40], and H_3PO_4 among others [41].

In addition, fixed-bed operation is required to acquire basic engineering data on the adsorbents for field operation. Fixed-bed sorption modes have been broadly utilized because of the benefits, for example, their possibility of in situ regeneration and simplicity of operation [42]. As an element of the demand for water, this method of operation can be utilized as a processing system of portable point of a use for a small community or a single household. Successful fixed-bed adsorption design and operation requires predictions of breakthrough curves (BTCs). Specific heat and mass

transfer processes and operating conditions in the adsorbent and column affect the nature of BTC [1, 43–45]. The optimal values for bed reduction time and regeneration time and bed height are determined by means of BTC. According to the work published by Ramutshatsha-makhwedzha et al. [24], it was observed that chemical activation of banana peels by H_2SO_4 activation agent increased the surface area of AC (600 °C) from 2.275 to 361.86 m^2/g, providing adequate properties for adsorption. The previous study done by Stavrinou et al. [46] investigated the case study on the adsorption of MB banana peels dried at a temperature of 100 °C. The sample utilized for adsorption was dried banana peels, without activation either by calcination or by activation agent. As predicted, the BET surface area of banana peel was low, as is typical of most agro- or carbonaceous materials [47]. Despite the limited surface area of BPAC, using H_2SO_4 (chemical activating agent), a porous structure is created by reconstructing the cellulose material's amorphous nature and aromatizing the carbon architecture [37].

Moreover, no study has been published on the column breakthroughs study using banana peels that was chemically activated using H_2SO_4 activation agent for the continuous removal of MB dye from wastewater effluents. This study highlights the importance of banana peels activated carbon (BPAC) material that was developed using H_2SO_4 activation agent in order to enhance the properties adsorbent for efficient adsorption. The yield of BPAC was examined on the packed-bed column using breakthrough curves. The effects of experimental variables like bed height, flow rate, and initial concentration of metal ions were studied. Moreover, the Yoon-Nelson and Thomas models were used to determine column parameters and to model the breakthrough curve that can be used in process design. Finally, to explore the real-world field performance of BPAC material in extracting MB, we collected environmental wastewater samples from laboratory at Tshwane University of Technology (TUT) in Pretoria West, South Africa.

2 Experimental

2.1 Materials and reagents

All standards and solutions were prepared using deionized water. Solutions and standards have been prepared using concentrated HNO_3 (65%, 15.7 M) from Sigma-Aldrich (Fluka, St. Louis, MO, USA). The glassware and polylactic container were washed and rinsed with 1% HNO_3 before they were thoroughly rinsed with distilled water before use. The MB was bought at Ace, Johannesburg, South Africa, and it was used to prepare a 1000-mg/L stock solution. The UV-vis instrument (Aqualytic AL800 Portable Spectrophotometer, Germany) was calibrated by analyzing the standard

solution at a concentration range of 1–150 mg/L. Banana peels had been gathered from the waste collection. Using a weak solution of NaOH or HNO₃, the pH of the solution was changed to the desired value.

2.2 Synthesis of the adsorbent (BPAC)

The preparation of activated banana peel waste has been modified after being taken from the literature [48]. Banana peels were gathered, cleaned, and oven-dried at 100° C. Using a pestle and a motor, the dried skin was ground into a fine powder. The powder was calcinated at 600° C in a furnace for 1 h. The sample was then activated at 1 M H_2SO_4 for 12 h. Samples were filtered and washed several times using distilled water until the pH of the water becomes neutral. The washed material was dried by an oven at 110 °C for 24 h and the final product achieved was used as an adsorbent (BPAC) for column study.

2.3 Characterization

X-ray diffraction (XRD) spectra were analyzed by a PANalytical X'Pert, X-ray diffractometer. The thermal behavior of generated BPAC was evaluated using a thermogravimetric analyzer (TGA) (4000, PerkinElmer, Inc. Waltham, USA) at a temperature range of 25 to 600 °C. The experiment was conducted in an inert (N_2) atmosphere using a tiny quantity of electrospun BPAC in a ceramic pan. Scanning electron microscopy-energy-dispersive X-ray spectroscopy was used to investigate the elemental compositions and morphologies of the prepared materials (SEM-EDS, TESCAN VEGA 3 XMU, LMH instrument, Czech Republic, Europe). The specific surface area and pore distributions of the materials were measured using N_2 adsorption/desorption isotherm ASAP 2020 TriStar II 3020 3.00 Analyzer (Micromeritics, Norcross, GA, USA). To determine the zeta potential, in 100-ml plastic bottles, 50 ml of deionized solutions with varying initial pH (2–9) was prepared. 0.1 g of BPAC was added in a solution and the mixture was shaken on an isothermal shaker at 25° C for 24 h. The graph of starting pH versus final pH-initial pH was plotted to get the pHpzc which is the point where $pH_{initial} = pH_{final}$.

2.4 Packed-bed column study

The performance of BPAC on the adsorption of MB dye from wastewater was evaluated using laboratory-scale packed-bed column experiments. A perspex glass tube-shaped container with a height of 30 cm and a 2-cm inner diameter was utilized as an adsorption column. The column was loaded with the adsorbent in the middle of the cotton wool and upheld by glass beads so that the solution flowed uniformly in the column. A peristaltic pump was used to pump the MB dye solution of known concentrations at pH 9 upward through the column at a desired flow rate and mass. The influent solution containing MB dye was pumped using an upwards mode to avoid channeling inside the column. The treated water which is wastewater sample was taken at a time interval and analyzed for MB concentration with a UV-vis spectrophotometer (Aqualytic AL800 Portable Spectrophotometer, Germany) at a wavelength of 664 nm. The theory of breakthrough curves serves as a representation of the packed-bed column's effectiveness. For column adsorption systems, these curves are crucial because they clearly show the breaking point, or the point at which the wastewater output concentration exceeds the maximum allowable release concentration of a specific water contaminant. The plot of exit concentration over time showed a breakthrough curve. Three main parameters (initial concentration, bed mass, and flow rate) that influence the shape of the breakthrough curve have been investigated to get the optimum behavior of the BPAC packed column.

2.5 Effect of initial concentration flow rate, and bed height

The study of continuous MB adsorption on BPAC adsorbent was investigated under various conditions. Experiments were performed at various initial feed concentrations (40, 80, and 120 mg/L), different flow rates (2, 5, and 10 mL/min), and different bed mass (1, 4, and 8 g) at a pH of 9. In each test conducted, one layer of the adsorbent bed was used, except when investigating the effect of bed height, where different bed mass was used. The initial MB feed solution was prepared with deionized water. The treated water samples were collected after a predetermined time and the residue was measured. The Treybal (1980) approach was adopted to calculate the column capacity to remove of MB dye [49]. Breakthrough capacity (50% or $C_i/C = 0.5$) is expressed in milligrams per liter of MB adsorbed in milligrams per gram of the adsorbent which was calculated according to Eq. 1.

$$\text{Breakthrough capacity} = \frac{\text{Feed Con.} \times \text{Breakthrough time} \times \text{Flow rate}}{\text{Mass of the adsorbent in bed (g)}} \quad (1)$$

2.6 Performance indicators

The volume of the beds plays a significant role in predicting how well the packed-bed column performs [50]. Adsorption efficiency is directly correlated with the number of bed volumes processed prior to the breakthrough point for a given bed mass. Equation provides the number of bed volumes processed to the breakthrough (2).

$$BV = \frac{\text{Volume of water treated at breakthrouth point (L)}}{\text{Volume of adsorbent (L)}}$$
(2)

Additionally, the frequency of adsorbent exchange can be calculated using the rate at which the adsorbent is depleted during adsorption. Equation provides the adsorption exhaustion rate (AER), where a low AER value indicates good bed performance (3).

$$AER = \frac{\text{Mass of adsorbent (g)}}{\text{Volume of water treated (L)}}$$
(3)

2.7 Fixed-bed adsorption studies using real wastewater

The real-world industrial applicability of BPAC composite was investigated using laboratory wastewater samples collected from TUT West Campus in Pretoria, South Africa. Collected wastewater samples were kept in laboratory polyethylene bottles for further analysis at 4° C, pH of 12, 93.3 NTU, and 9.82 mS. The fixed-bed adsorption experiments were performed on wastewater samples using the optimal conditions and the procedures were described in Section 2.6. The experiments were performed with a bed mass of 8 g and an inlet flow rate of 2 mL/min, and the behavior of MB breakthrough was monitored.

2.8 Adsorption and desorption studies

Desorption experiments were performed using a bed depth of 96 mm, an influent flow rate of 2 mL/min, and a MB concentration of 40 mg/L. After the bed is exhausted in the first cycle, 3 M HNO_3 acid was used to flush solution until the concentration of MB in the effluent remains almost unchanged. The choice of eluent was influenced by the surface of each sorbent which becomes protonated under acidic conditions, allowing the desorption of cations [51]. The bed was washed with deionized water after every cycle until the pH of the effluent was neutral. The adsorption-desorption process was repeated five times and the percentage removal for each cycle was calculated.

3 Results and discussions

3.1 Characterization of the adsorbent

XRD was utilized to affirm the crystalline stage and microstructure of the synthesized BPAC. Figure 1 indicates the XRD designs of BPAC that were examined by scanning the 2-theta range from 5.00 to 90.00. The BPAC design shows amorphous structure of the material with broader
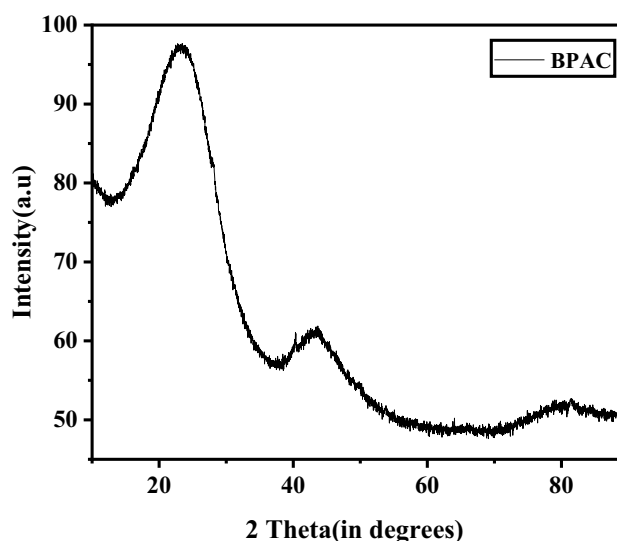

Fig. 1 XRD spectrum of BPAC

peak from 19 to 30°. Same results were observed and reported on the literature [34, 35, 52, 53].

Figure 2 shows the TGA results from BPAC before adsorption. The BPAC's raw material degradation takes place in three stages. Evaporation of water leads to an initial loss of weight (3%) up to 50 °C. The thermal decomposition of hemicellulose and cellulose produces weight loss of 8% that ranged in temperature from 50 to 150 °C [54]. Degradation appears above 150°C due to the concentration of lignin, a stable structure. The thermal degradation of BPAC, however, after MB adsorption starts around 50 °C and can extend up to 500 °C. This material shows good thermal stability.
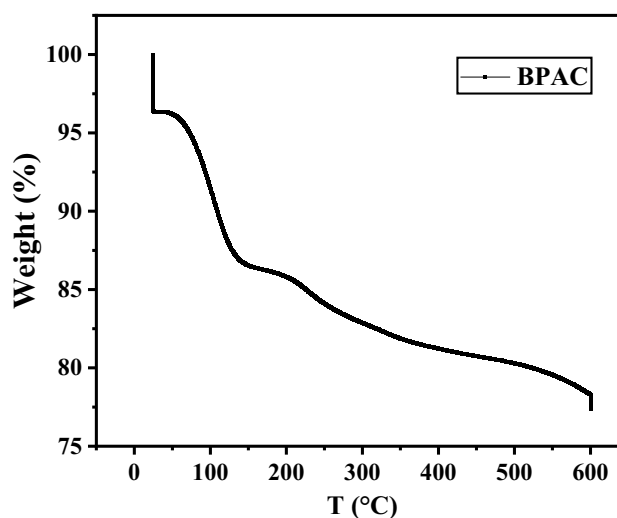

Fig. 2 TGA spectrum of BPAC

Figure 3 exhibits the SEM-EDS morphological structure and the composition of BPAC materials. The results of the SEM image in Fig. 3 a appear to show a BPAC structure connected to one another with formation of cavities on the materials surface that took after the arrangement of pores [22]. This permeable structure permits productive adsorption because it offers satisfactory free spaces for target adsorbates [55]. The EDS range of the prepared material affirmed the presence of primarily C, 88.9%, and O, 16.9%, by weight (Fig. 3b).

Figure 4 portrays the N_2 adsorption-desorption isotherms of BPAC material. The isotherms in Fig. 4 show a sort IV isotherm with a H1 hysteresis circle, demonstrating that the adsorbent is mesoporous in nature [56]. The BET pore volume and surface area were viewed as 0.2294 m^3/g and 361 m^2/g, respectively. The large surface area attained is good for adsorption interaction since it offers more active sites for reaction to occur. The zeta potential of BPAC (pHpzc) was found to be 2.5. This suggests that the adsorbent's surface charge is positive below pHpzc and negative above it. Additionally, the adsorbent becomes negatively charged when the solution's pH rises above pHpzc that boost electrostatic interactions between the cationic MB and the negatively charged BPAC.

3.2 Breakthrough curve modeling

This section evaluates the key parameters in column design, such as initial feed concentration, bed mass, and flow rate. Additionally, numerous mathematical models that were advanced to explain and examine laboratory-scale columns of studies with experimental data are prepared for industrial applications.
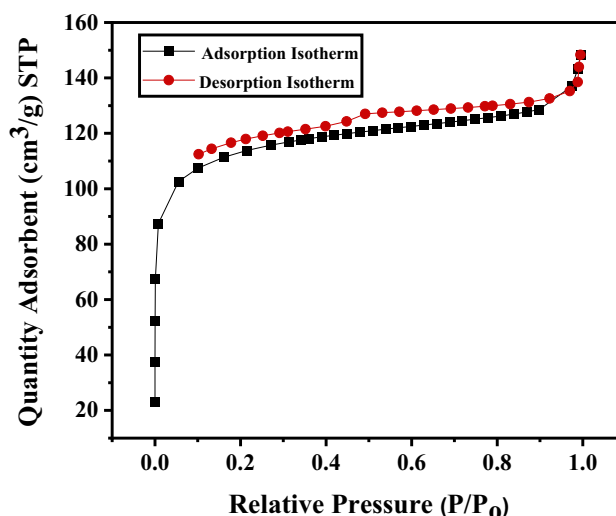
Fig. 4 Nitrogen adsorption-desorption curve for BPAC

3.2.1 Effect of bed mass

Since the particles adsorbed are subject to the active sites available for adsorption, the bed mass is a crucial boundary in sorption processes. The flow rate and influent concentration were kept constant at 2 mL/min and 80 mg/L, respectively, while bed mass was varied to determine the effect of bed mass on MB sorption (1, 4, and 8 g). Figure 5 displays the breakthrough curves of MB sorption at various bed masses. As noticed, the breakthrough curve increments were from 80 to 250 min with expanding bed mass from 1 to 8 g, and due to the small mass of the bed, there are fewer active sites where MB is adsorbed. Therefore, the adsorbent saturates faster, resulting in earlier breakthrough point. On the contrary, there is a higher bedding mass resulting to more active sites for adsorption; thus, an increase in depletion

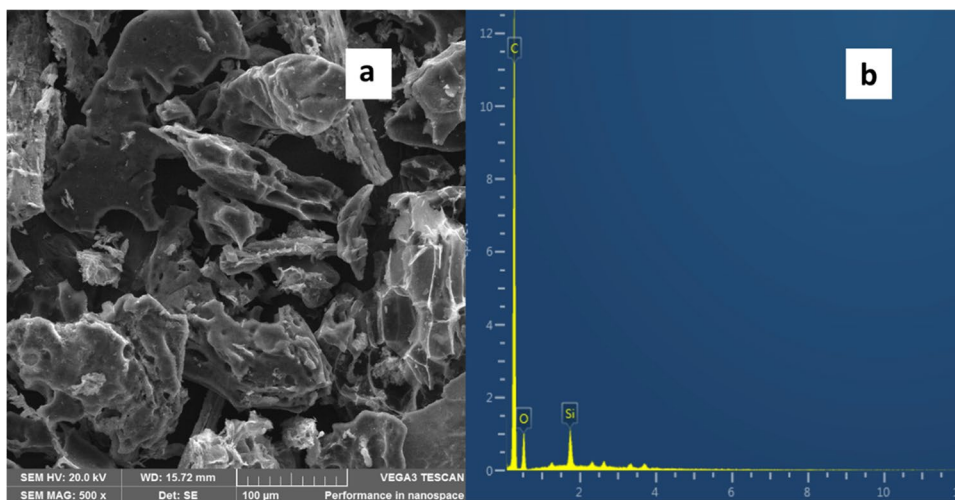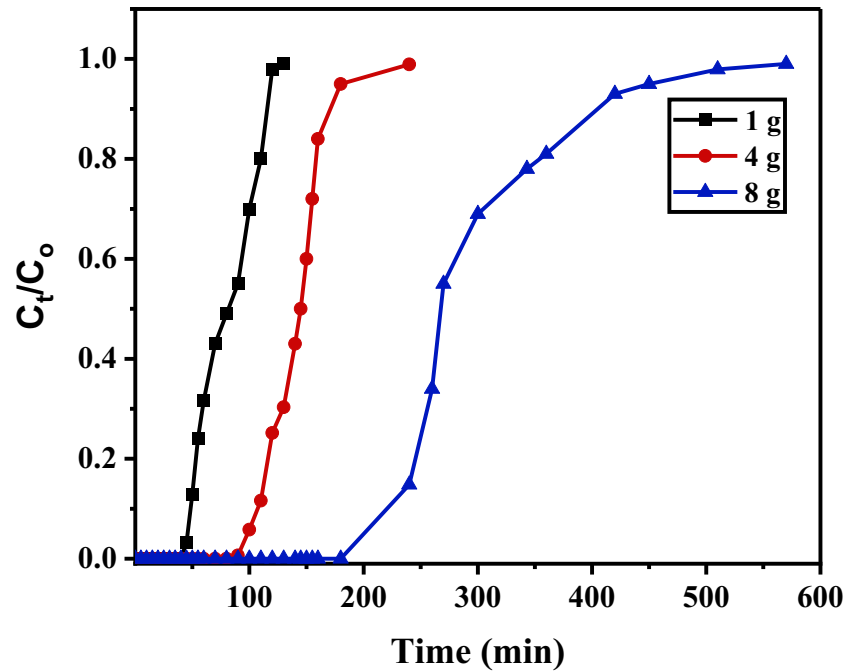**Fig. 3** **a** SEM image and **b** EDS spectrum of BPAC

Fig. 5 Effect of mass of adsorbent on the breakthrough curve for removal of MB using BPAC (initial concentration 80 mg/L, flow rate 2 mL/min) and pH of 9

time is also observed leading to slower breakthrough time and a larger amount of treated water [42]. Also, a shorter bed height or low bed mass has axial dispersion general mass transfer phenomena that occur automatically to decreases the radial diffusion in metal ions. Compared with the longer the bed, the wider the mass transfer zone, the more the collection sites are present for adsorption [57]. Table 1 shows the MB ions adsorbed at breakthrough and exhaustion times.

### 3.2.2 Effect of initial MB concentration

The initial focus for breakthrough curve performance is shown in Fig. 6. To demonstrate how well BPAC adsorbs MB in a continuous fixed-bed column, three different initial concentrations of 40, 80, and 120 mg/L were used. Three milliliters/min flow rate and 5 g bed mass were maintained constants. The breakthrough at 50% was 180 min, 250 min, and 500 min for 40, 80, and 120 mg/L. The breakthrough time decreased with increasing initial MB concentration; because of this, less water is treated at breakthrough points. At increased initial concentration, higher driving force for mass transfer accelerates the saturation of the adsorbent sorption site, thus shortening adsorption time [50]. Consequently, as the concentration rises, MB increases loading rate as well as mass transfer propulsion, where the length of the adsorption zone is reduced [58]. When the initial concentration increases from 40 to 120 mg/L, the AER values increased from 7.22 to 22.22 g/L (Table 1). The results suggested that MB removal by BPAC on fixed bed is appropriate at low concentration.

Table 1 Parameters for breakthrough curve

Adsorbent mass (g)	tb	Volume processed (L)	AER (g/L)	Breakthrough capacity (mg/g)	EBCT (min)	Bed volume
1	80	0.16	6.25	12.8	13.587	27.174
4	145	0.29	13.79	5.8	7.902	15.804
8	260	0.52	15.38	5.2	7.819	15.639
Initial concentration (mg/L)						
40	510	1.02	7.83	5.1	15.693	31.385
80	260	0.52	15.38	5.2	7.819	15.639
120	180	0.36	22.22	5.4	5.537	11.074
Flow rate (mL/min)						
2	510	1	8.00	5.1	15.380	30.759
5	260	1.3	6.15	6.5	7.998	39.988
7	145	0.7	11.43	3.6	3.076	21.532

Fig. 6 Effect of initial concentration on the breakthrough curve for removal of MB using BPAC (bed mass 8 g), flow rate 2 mL/min, and pH of 9
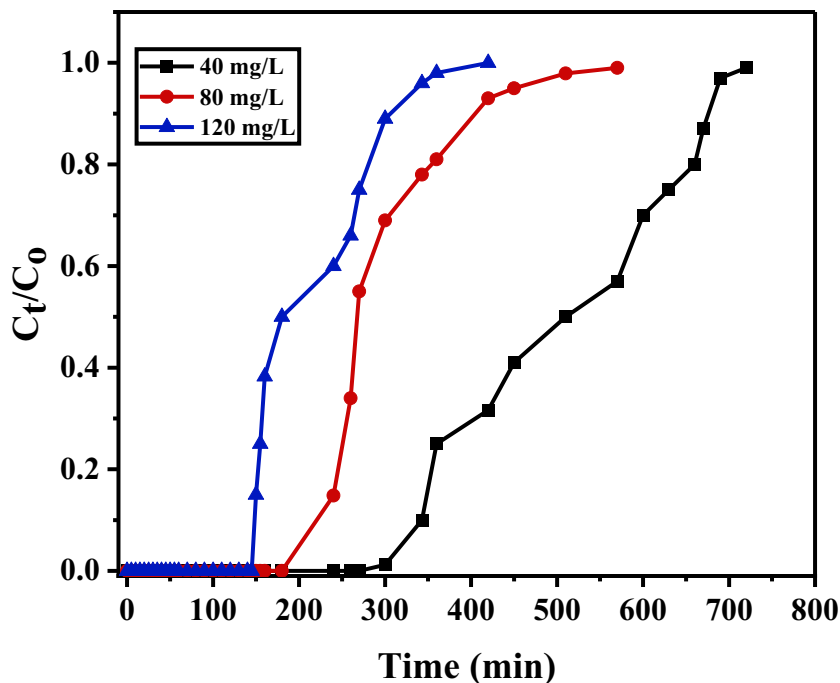

3.2.3 Effect of flow rate dye concentration

The effect of the flow rate was investigated by changing the flow rate from 1.0 to 3.0 mL/min at constant bed mass of 80 g and MB concentration of 40 mg/L. Figure 7 shows the breakthrough curve of C_{out}/C_{in} and the relationship with the time when the flow rate is changed. It was shown

that reducing the flow rate when the bed height is constant increases the breakthrough time (tb). Breakthrough time (50%) was 100 min, 270 min, and 450 min at a flow rate of 2.0, 5.0, and 7.0 ml/min, respectively. The inflow rate was inversely proportional to both tb and bed saturation time (t_s); the bed saturates faster at higher flow rates than low flow rates. As shown in Table 1, the t_s of 2, 5, and 7 mL/min were

Fig. 7 Effect of flow rate on the breakthrough curve for removal of MB using BPAC (adsorbent bed 8g), pH of 9, and initial concentration 40 mg/L
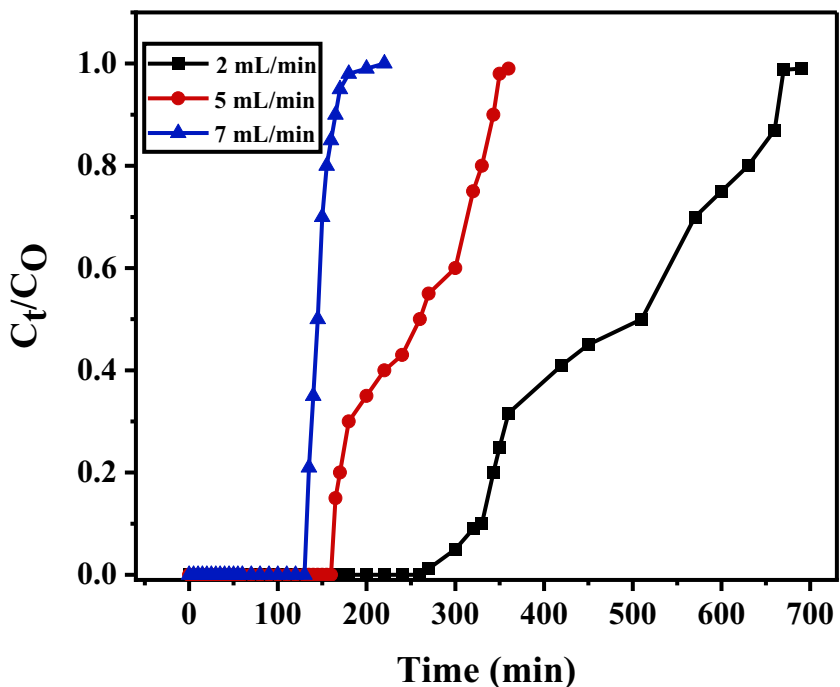
200, 340, and 700 min, respectively. Because at high inflow, contact time between adsorbent and MB is short. This phenomenon can be explained by the basic principles of mass transfer where convection can occur through mass transfer rate control mechanism at higher flow rate evaluation [50].

3.3 Statistic analysis

T-test analysis was used to determine the significance of the independent variables and their interactions. To represent the statistical significance of the quadratic model, the results were examined using several descriptive statistics such as *p*-value, standard error mean (SEM), degrees of freedom, *t*-statistics, mean, and standard deviation test. To analyze the association between the validation data and the associated model projected responses, *t*-tests were used to validate the model. The one-pair *t*-test and *p*-values in Table S1 were used to determine the significance of the quadratic model coefficients. The *t*-value is the ratio of the estimated parameter impact to the standard deviation of the estimated parameter. The *p*-value is a method for determining the importance of a coefficient. The more significant the relevant parameter in the regression model, the bigger the magnitude of the *t*-value and the smaller the *p*-value. Table S1 shows that all the linear terms are statistically significant ($p < 0.05$) and the null hypothesis was rejected.

3.4 Modeling of breakthrough curve

Successful continuous adsorption separation unit design needs prior design information collected through various experiments to establish conditions for optimal performance. To save time and money through a series of experiments, important design information needs to be collected, and models are commonly applied to predict ideal conditions.

3.4.1 Thomas model

The Thomas model is a very common model applied to predict BTC and describes the performance of fixed-bed columns. This is derived as a function of the second-order reaction rate and assumes that the chemical reaction does not limit sorption; rather, mass transfer and chemical reaction at the interface do [59]. This model calculates the maximum solute adsorption capacity onto adsorbent as well as the rate constant in the column, which is required in the design of a fixed-bed column. Equation 3 expresses the Thomas model.

$$\ln\left(\frac{C_O}{C_t} - 1\right) = \frac{k_{Tq_o}x}{V} - k_T C_O t \tag{3}$$

where k_T is the rate constant of dynamic adsorption by the Thomas model (mL mg^{-1} min^{-1}) and q_o is the total adsorption capacity calculated using the Thomas model (mg/g), and t is the time (min). The Thomas constants (q_{th} and k_T) are estimated on plot $\ln(C_o/C_t - 1)$ vs t using non-linear regression. The linear regression coefficient has a high value ($R_2 > 0.9$) in Table 2 which demonstrated that such a model fits the experimental data properly. When the flow rate was increased, the magnitude of q_e decreased rapidly while k_T increased. The k_T decreased as the bed depth increased, but q_e increased.

3.4.2 Yoon-Nelson model

The Yoon-Nelson model is used for interpreting the behavior of the MB breakthrough with respect to BPAC. The main presumption of this model is that the rate of decrease in the adsorption probability of an adsorbent molecule is proportional to the likelihood of adsorption of the adsorbent and the likelihood of breakthrough of the adsorbent to the adsorbent. The linear plot of $\ln(C_e/C_o - C_e)$ vs t was used to

Table 2 Yoon-Nelson and Thomas model parameters for adsorption of MB on BPAC

Adsorbent mass (g)	Thomas model			Yoon-Nelson model		
	$K_{th} \times 10^{-5}$ (mL min^{-1} mg)	q_o (mg/g)	R^2	k_{YN}	t (min)	R^2
1	2.20	798,054.054	0.8927	0.1777	62.31	0.8927
4	5.00	1,942,565.00	0.8972	0.1361	125.55	0.9731
8	25.00	1,575,145.63	0.9663	0.0206	302.93	0.9663
MB initial concentration (mg/L)						
40	33.25	1,684,112.90	0.9712	0.0096	501.59	0.9767
80	25.00	1,575,145.63	0.9663	0.0206	302.93	0.9663
120	22.30	1,155,608.06	0.9174	0.0249	211.47	0.9876
Flow rate mL/min						
2	31.25	1,684,112.90	0.9712	0.0096	501.59	0.9767
5	4.00	1,644,906.25	0.9366	0.0157	247.05	0.9630
7	5.00	505,462.687	0.9933	0.1341	144.31	0.9933

discover the Yoon-Nelson model constant, k_{YN} (min), and the time needed at 50 % adsorbate breakthrough (min) [46].

$$\ln\left(\frac{C_t}{C_o - C_t}\right) = k_{YN}t - \tau k_{YN} \tag{4}$$

where τ is the required time at 50% adsorbate breakthrough and k_{YN} is the Yoon-Nelson rate constant (min). The fact that the value of τ depends on time suggests that it has no potential to affect the BTC. It is common practice to determine the values of k_{YN} and from the linear slope of ln [C_t/($C_o - C_t$)] versus t. The results demonstrate that the values of k_{YN} increase with the rise in concentration and decrease in adsorbent mass. The breakthrough curve was predicted using the model's obtained parameters (Table 2). The obtained experimental data were well represented by the Yoon-Nelson model.

3.5 Removal of MB dye from wastewater

The application of BPAC adsorbent for MB dye removal from environmental water was tested on contaminated laboratory water samples collected from the TUT Pretoria West Campus, South Africa. Figure 8 depicts the breakthrough study that was obtained using a bed mass of 8.0 g and a flow rate of 2 mL/min. The breakthrough time of BPAC on MB dye was found to be 580, and bed exhaustion time of 800 min, respectively. The volume of water treated at breakthrough was 1.16 L, which corresponds to the AER of 240 g/L, and the overall volume treated and BV were found to be 1.60 and 34.89 L at during breakthrough time. The results confirmed high affinity of BPAC material for MB, which can be attributed to the negatively charged MB dye, as confirmed by pH$_{pzc}$.

The literature review shows that the metal adsorption limits of ACs made from different materials are very diverse. Table 3 lists the maximum adsorption capacities for MB, which range from 126 to 6.7 mg/g [41, 60–63], respectively; the BPAC data analyzed was comparable to the available literature.

3.6 Regeneration study

Regeneration and desorption studies are conducted: first, to protect the environment from secondary contamination because of the removal of adsorbent that has been loaded with metals. Second, to determine economics of adsorption processes by recovering adsorbed species and recycling adsorbents. The usual method involves a cyclic adsorption-desorption operations. Figure 9 shows the desorption curves after five repeated adsorption-desorption cycles using the eluent 3 M HNO$_3$ (pH 9). The results showed that desorption process was simple, requiring only a part of the bed emptying time for each up to the third, and the BPAC adsorbent can be reused to the fourth cycles without much loss in capacity.

Fig. 8 Breakthrough profile of MB dye removal from wastewater by BPAC adsorbent (pH = 12; flow rate = 2 mL/min; initial concentration = 30 mg/L; bed mass = 8.0 g)
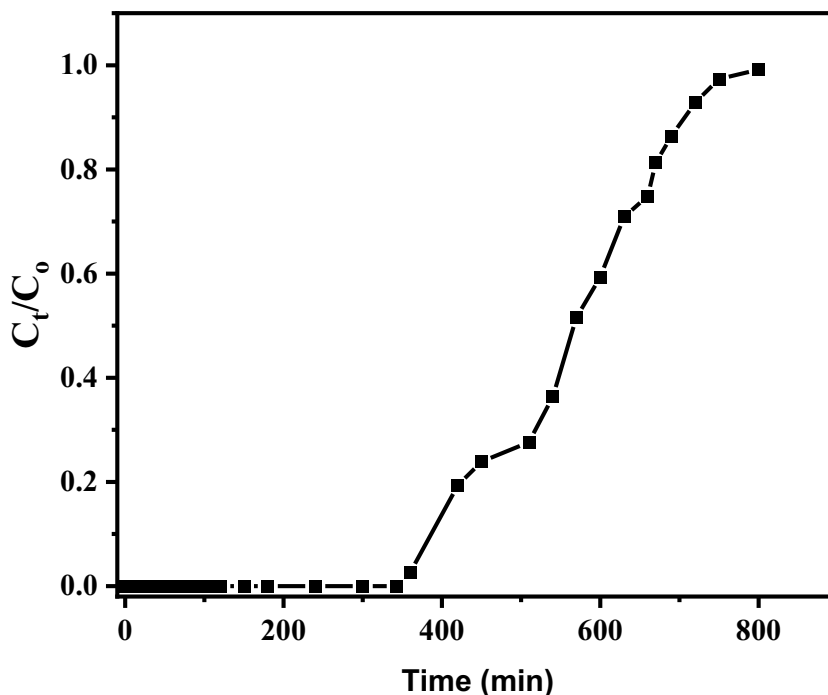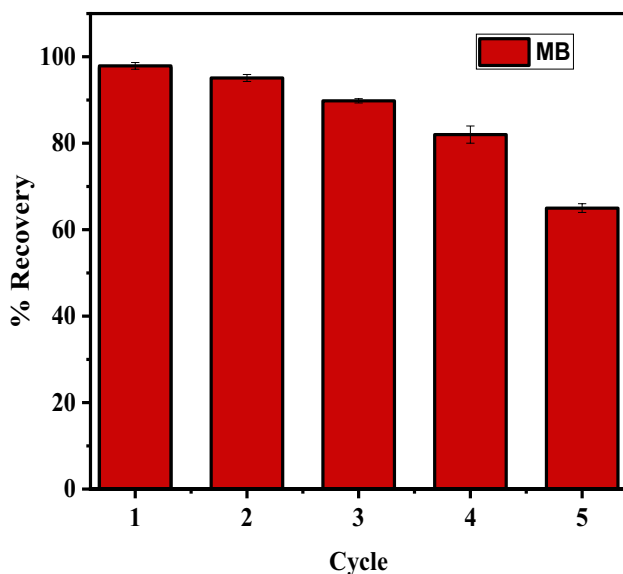
Table 3 Comparison of adsorption at column equilibrium capacities of various adsorbents using BPAC material

Adsorbent	Influent concentration mg/L	pH	Capacity (mg/g)	Ref.
H_3PO_4 activated carbon fibers	15	5.5	126	[41]
Eucalyptus Sheathiana	100	7.5	49.55	[60]
Composite citrus peel-alginate	200	6.3	31.45	[61]
Mesoporous silica Microporous silica	50	6	6.7 10.4	[62]
Alginate-activated carbon	300	6.7	51.75	[63]
Waste BPAC	40	9	5.1	This work

Fig. 9 Adsorption-desorption studies

The BPAC material was used in wastewater samples for the removal of MB dye. The BPAC breakthrough time to MB was 580 min and bed exhaustion time was 800 min, respectively. The amount of water treated at breakthrough was 1.16 L, like an AER of 240 g/L. Studies on environmental wastewater indicated that a packed-bed column of BPAC sorbent material has great potential for MB remediation. The BPAC material can be recovered for up to 4 cycles with percentage removal of >80%. These can be said to be excellent purification technologies for adsorption of MB

Declarations

4 Conclusion

In this work, banana peel-activated carbon (BPAC) material was synthesized, characterized, and analyzed for continuous removal of MB dye from wastewater through a packed-bed column. The study found that activated carbon generated from banana peel could be employed as an adsorbent for MB from wastewater. The chemical activation approach yielded the large active surface carbon (361.86 m^2/g from 1 M H_2SO_4). The BPAC adsorbent material demonstrated good thermal stability with the final temperature of 500 °C.

BPAC adsorbent had properties such as interconnected structure which resembles high porosity. The XRD shows amorphous phase of BPAC with broader peaks. Breakthrough study was highly dependent on process variables such as concentration, bed mass, and inlet flow rate. The nonlinear regression showed that the breakthrough experimental data fitted Thomas and Yoon-Nelson models well.

References

1. El-Shamy AG (2020) An efficient removal of methylene blue dye by adsorption onto carbon dot @ zinc peroxide embedded poly vinyl alcohol (PVA/CZnO$_2$) nano-composite: a novel Reusable adsorbent. Polymer (Guildf) 202:122565. https://doi.org/10.1016/j.polymer.2020.122565

2. Bharathi D, Nandagopal JGT, Ranjithkumar R, Gupta PK, Djearamane S (2022) Microbial approaches for sustainable remediation of dye-contaminated wastewater: a review. Arch Microbiol 204(3):1–11. https://doi.org/10.1007/s00203-022-02767-3

3. Hasanin MS (2020) Sustainable hybrid silica extracted from rice husk with polyvinyl alcohol and nicotinic acid as multi adsorbent for textile wastewater treatment. Environ Sci Pollut Res 27(21):26742–26749. https://doi.org/10.1007/s11356-020-09104-5

4. Rameshkumar S, Henderson R, Padamati RB (2020) Improved surface functional and photocatalytic properties of hybrid zno-mos2-deposited membrane for photocatalysis-assisted dye filtration. Membranes (Basel) 10(5). https://doi.org/10.3390/membranes10050106

5. Ebrahim SE, Mohammed TJ, Oleiwi HO (2018) Removal of acid blue dye from industrial wastewater by using reverse osmosis technology. Assoc Arab Univ J Eng Sci 25(3):29–40 https://www.jaaru.org/index.php/auisseng/article/view/165

6. Zhang J, Huang GQ, Liu C, Zhang RN, Chen XX, Zhang L (2018) Synergistic effect of microbubbles and activated carbon on the ozonation treatment of synthetic dyeing wastewater. Sep Purif Technol 201:10–18. https://doi.org/10.1016/j.seppur.2018.02.003

7. Guesmi Y, Agougui H, Lafi R, Jabli M, Hafiane A (2018) Synthesis of hydroxyapatite-sodium alginate via a co-precipitation technique for efficient adsorption of Methylene Blue dye. J Mo Liq 249:912–920. https://doi.org/10.1016/j.molliq.2017.11.113

8. Naushad M, Alqadami AA, AlOthman ZA, Alsohaimi IH, Algamdi MS, Aldawsari AM (2019) Adsorption kinetics, isotherm and reusability studies for the removal of cationic dye from aqueous medium using arginine modified activated carbon. J Mol Liq 293:111442. https://doi.org/10.1016/j.molliq.2019.111442

9. Aqeel K et al (2020) Electrochemical removal of brilliant green dye from wastewater. IOP Conf Ser Mater Sci Eng 888(1). https://doi.org/10.1088/1757-899X/888/1/012036

10. Saxena M, Sharma N, Saxena R (2020) Highly efficient and rapid removal of a toxic dye: adsorption kinetics, isotherm, and mechanism studies on functionalized multiwalled carbon nanotubes. Surf Interfaces 21:100639. https://doi.org/10.1016/j.surfin.2020.100639

11. Hashem AH, Saied E, Hasanin MS (2020) Green and ecofriendly bio-removal of methylene blue dye from aqueous solution using biologically activated banana peel waste. Sustain Chem Pharm 18:100333. https://doi.org/10.1016/j.scp.2020.100333

12. Kheirabadi M et al (2019) Well-designed Ag/ZnO/3D graphene structure for dye removal: adsorption, photocatalysis and physical separation capabilities. J Colloid Interface Sci 537:66–78. https://doi.org/10.1016/j.jcis.2018.10.102

13. Mariyam A, Mittal J, Sakina F, Baker RT, Sharma AK, Mittal A (2021) Efficient batch and fixed-bed sequestration of a basic dye using a novel variant of ordered mesoporous carbon as adsorbent. Arab J Chem 14(6):103186. https://doi.org/10.1016/j.arabjc.2021.103186

14. Ramutshatsha-makhwedzha D, Mavhungu A, Moropeng ML, Mbaya R (2022) Activated carbon derived from waste orange and lemon peels for the adsorption of methyl orange and methylene blue dyes from wastewater. Heliyon 8:e09930. https://doi.org/10.1016/j.heliyon.2022.e09930

15. Li W, Mu B, Yang Y (2019) Bioresource Technology feasibility of industrial-scale treatment of dye wastewater via bio- adsorption technology. Bioresour Technol 277:157–170. https://doi.org/10.1016/j.biortech.2019.01.002

16. D. Lin et al., "Adsorption of dye by waste black tea powder : parameters , kinetic , equilibrium , and thermodynamic studies". vol. 2020, 2020

17. Hami HK, Abbas RF, Eltayef EM, Mahdi NI (2021) Applications of aluminum oxide and nano aluminum oxide as adsorbents: review. Samarra J Pure Appl Sci 2(2):19–32. https://doi.org/10.54153/sjpas.2020.v2i2.109

18. Munonde TS, September NP, Mpupa A, Nomngongo PN (2022) Two agitation routes for the adsorption of Reactive Red 120 dye on NiFe LDH/AC nanosheets from wastewater and river water. Appl Clay Sci 219:106438. https://doi.org/10.1016/j.clay.2022.106438

19. Molavi H, Shojaei A, Pourghaderi A (2018) Rapid and tunable selective adsorption of dyes using thermally oxidized nano-diamond. J Colloid Interface Sci 524:52–64. https://doi.org/10.1016/j.jcis.2018.03.088

20. de Souza TNV, de Carvalho SML, Vieira MGA, da Silva MGC, Brasil DDSB (2018) Adsorption of basic dyes onto activated carbon: experimental and theoretical investigation of chemical reactivity of basic dyes using DFT-based descriptors. Appl Surf Sci 448:662–670. https://doi.org/10.1016/j.apsusc.2018.04.087

21. Wang H et al (2020) Effective adsorption of dyes on an activated carbon prepared from carboxymethyl cellulose: experiments, characterization and advanced modelling. Chem Eng J 417:128116. https://doi.org/10.1016/j.cej.2020.128116

22. Thabede PM, Shooto ND, Naidoo EB (2020) Removal of methylene blue dye and lead ions from aqueous solution using activated carbon from black cumin seeds. South African J Chem Eng 33:39–50. https://doi.org/10.1016/j.sajce.2020.04.002

23. Herrera-González AM, Caldera-Villalobos M, Peláez-Cid AA (2019) Adsorption of textile dyes using an activated carbon and crosslinked polyvinyl phosphonic acid composite. J Environ Manage 234:237–244. https://doi.org/10.1016/j.jenvman.2019.01.012

24. Ramutshatsha-Makhwedzha D, Mbaya R, Mavhungu ML (2022) Application of activated carbon banana peel coated with Al$_2$O$_3$-chitosan for the adsorptive removal of lead and cadmium from wastewater. Materials (Basel) 15(3). https://doi.org/10.3390/ma15030860

25. Abdelkhalek A, Ali SSM, Sheng Z, Zheng L, Hasanin M (2022) Lead removal from aqueous solution by green solid film based on cellulosic fiber extracted from banana tree doped in polyacrylamide. Fibers Polym 23(5):1171–1181. https://doi.org/10.1007/s12221-022-4001-y

26. Rehali H, Elbar D, Ghiaba L, Bounafi K (2021) Elimination of nickel (II) in water with different activated carbons (dates nut, peach nuts and apricot kernels). Dig J Nanomater Biostructures 16(1):109–118

27. Info A (2019) Study of the adsorption of methylene blue by natural materials (olive stone, date pit and their mixture) in fixed bed column. Int J Environ Sci Technol (Tehran) 5:947–954

28. Liu L, Fan S, Li Y (2018) Removal behavior of methylene blue from aqueous solution by tea waste: kinetics, isotherms and mechanism. Int. J. Environ. Res. Public Health 15(7). https://doi.org/10.3390/ijerph15071321

29. Enniya I, Rghioui L, Jourani A (2017) Adsorption of hexavalent chromium in aqueous solution on activated carbon prepared from apple peels. Sustain Chem Pharm 7:9–16. https://doi.org/10.1016/j.scp.2017.11.003

30. Aljeboree AM, Al-Baitai AY, Abdalhadi SM, Alkaim AF (2021) Investigation study of removing methyl violet dye from aqueous solutions using corn-cob as a source of activated carbon. Egypt J Chem 64(6):2873–2878. https://doi.org/10.21608/ejchem.2021.55274.3159

31. Pagalan E et al (2019) Activated carbon from spent coffee grounds as an adsorbent for treatment of water contaminated by aniline yellow dye. Ind Crops Prod 145:111953. https://doi.org/10.1016/j.indcrop.2019.111953

32. Pandiarajan A, Kamaraj R, Vasudevan S, Vasudevan S (2018) OPAC (orange peel activated carbon) derived from waste orange peel for the adsorption of chlorophenoxyacetic acid herbicides from water: adsorption isotherm, kinetic modelling and thermodynamic studies. Bioresour Technol 261(April):329–341. https://doi.org/10.1016/j.biortech.2018.04.005

33. Benjelloun M, Miyah Y, Akdemir G, Zerrouq F, Lairini S (2021) Recent advances in adsorption kinetic models : their application to dye types. Arab J Chem 14(4):103031. https://doi.org/10.1016/j.arabjc.2021.103031

34. Thomas B, Alexander EPSLK (2021) Role of functional groups and morphology on the pH - dependent adsorption of a cationic dye using banana peel , orange peel , and neem leaf bio – adsorbents. Emerg Mater Res 4(5):1479–1487. https://doi.org/10.1007/s42247-021-00237-y

35. Mohammadifard A, Allouss D, Vosoughi M, Dargahi A, Moharrami A (2022) Synthesis of magnetic Fe_3O_4 / activated carbon prepared from banana peel (BPAC@Fe_3O_4) and salvia seed (SSAC @Fe_3O_4) and applications in the adsorption of Basic Blue 41 textile dye from aqueous solutions. Appl Water Sci 12(5):1–11. https://doi.org/10.1007/s13201-022-01622-6

36. Science E Equilibrium kinetic and isotherm studies of dye colour adsorption on the banana peel equilibrium kinetic and isotherm studies of dye colour adsorption on the banana peel. https://doi.org/10.1088/1755-1315/920/1/012029

37. Devarajan Y, Lakshmaiya N (2022) Effective utilization of waste banana peel extracts for generating activated carbon-based adsorbent for emission reduction. Biomass Convers Biorefinery:0123456789. https://doi.org/10.1007/s13399-022-03470-5

38. Tadesse MG, Kasaw E, Lübben JF (2023) Valorization of banana peel using carbonization: potential use in the sustainable manufacturing of flexible supercapacitors. Micromachines 14(2). https://doi.org/10.3390/mi14020330

39. Yuliusman JS, Nugroho YW, Naf'an HI (2018) Preparation of activated carbon from banana peel waste as adsorbent for motor vehicle exhaust emissions. E3S Web Conf 67:1–6. https://doi.org/10.1051/e3sconf/20186703020

40. Gupta V, Dave S, Parihar N (2020) Removal of copper (II) from aqueous solution using chemically activated banana peels as an adsorbent. 39(2):287–291

41. Silva MC et al (2021) H3PO4–activated carbon fibers of high surface area from banana tree pseudo-stem fibers: adsorption studies of methylene blue dye in batch and fixed bed systems. J Mol Liq 324. https://doi.org/10.1016/j.molliq.2020.114771

42. Ramutshatsha-Makhwedzha D, Ndungu PG, Nomngongo PN (2022) Adsorptive removal of major and trace metal ions from synthetic saline and real seawater samples onto magnetic zeolite nanocomposite: application of multicomponent fixed-bed column adsorption. J Iran Chem Soc:0123456789. https://doi.org/10.1007/s13738-022-02506-x

43. Charola S, Yadav R, Das P, Maiti S (2018) Fixed-bed adsorption of Reactive Orange 84 dye onto activated carbon prepared from empty cotton flower agro-waste. Sustain Environ Res 28(6):298–308. https://doi.org/10.1016/j.serj.2018.09.003

44. Parimelazhagan V, Jeppu G, Rampal N (2022) Continuous fixed-bed column studies on congo red dye adsorption-desorption using free and immobilized nelumbo nucifera leaf adsorbent. Polymers (Basel) 14(1). https://doi.org/10.3390/polym14010054

45. Kannan P, Pal P, Banat F (2020) Design of adsorption column for reclamation of methyldiethanolamine using homogeneous surface diffusion model. Oil Gas Sci Technol 75. https://doi.org/10.2516/ogst/2020073

46. Stavrinou A, Aggelopoulos CA, Tsakiroglou CD (2020) A methodology to estimate the sorption parameters from batch and column tests: the case study of methylene blue sorption onto banana peels. Processes 8(11):1–22. https://doi.org/10.3390/pr8111467

47. Maia LS, Duizit LD, Pinhatio FR, Mulinari DR (2021) Valuation of banana peel waste for producing activated carbon via NaOH and pyrolysis for methylene blue removal. Carbon Lett 31(4):749–762. https://doi.org/10.1007/s42823-021-00226-5

48. Gupta H, Kumar R (2016) Removal of PAH anthracene from aqueous media using banana peel activated carbon. Int J Sci Res Environ Sci 4(4):109–114. https://doi.org/10.12983/ijsres-2016-p0109-0114

49. T. R.E., Mass - Transfer Operations R . E . Treybal Scilab Textbook Companion for Mass - Transfer Operations. 1980

50. Muliwa AM, Leswifi TY, Maity A, Ochieng A, Onyango MS (2018) Fixed-bed operation for manganese removal from water using chitosan/bentonite/MnO composite beads. Environ Sci Pollut Res 25(18):18081–18095. https://doi.org/10.1007/s11356-018-1993-3

51. Bogusz A, Oleszczuk P, Dobrowolski R (2015) Application of laboratory prepared and commercially available biochars to adsorption of cadmium, copper and zinc ions from water. Bioresour Technol 196:540–549. https://doi.org/10.1016/j.biortech.2015.08.006

52. Lee SM, Lee SH, Roh JS (2021) Analysis of activation process of carbon black based on structural parameters obtained by XRD analysis. Crystals 11(2):1–11. https://doi.org/10.3390/cryst11020153

53. Abu Bakar AA, Pauzi AM, Mohamed AA, Idris FM, Yazid H (2019) Preliminary analysis of gamma and neutron irradiation on sand and activated carbon by using SEM, XRD and SAXS. IOP Conf Ser Mater Sci Eng 555(1). https://doi.org/10.1088/1757-899X/555/1/012024

54. Ramutshatsha D, Tresor M, Avhafunani M, Mapula M, Mavhunga L (2023) Adsorptive removal of Cd^{2+},Pb^{2+}, and Fe^{2+} from acid mine drainage using a mixture of waste orange and lemon activated carbon (WOLAC): equilibrium study. J Iran Chem Soc:0123456789. https://doi.org/10.1007/s13738-022-02739-w

55. Akawa MN, Dimpe KM, Nomngongo PN (2021) An adsorbent composed of alginate, polyvinylpyrrolidone and activated carbon (AC@PVP@alginate) for ultrasound-assisted dispersive micro-solid phase extraction of nevirapine and zidovudine in environmental water samples. Environ Nanotechnol Monit Manag 16:100559. https://doi.org/10.1016/j.enmm.2021.100559

56. Nasrullah A, Bhat AH, Naeem A, Hasnain M (2018) High surface area mesoporous activated carbon-alginate beads for efficient removal of methylene blue. Int J Biol Macromol 107:1792–1799. https://doi.org/10.1016/j.ijbiomac.2017.10.045

57. Patel H (2020) Batch and continuous fixed bed adsorption of heavy metals removal using activated charcoal from neem (Azadirachta indica) leaf powder. Sci Rep 10(1):1–12. https://doi.org/10.1038/s41598-020-72583-6

58. Khalfa L, Sdiri A, Bagane M, Cervera ML (2021) A calcined clay fixed bed adsorption studies for the removal of heavy metals from aqueous solutions. J Clean Prod 278:123935. https://doi.org/10.1016/j.jclepro.2020.123935

59. Alardhi SM, Albayati TM, Alrubaye JM (2020) Adsorption of the methyl green dye pollutant from aqueous solution using mesoporous materials MCM-41 in a fixed-bed column. Heliyon 6(1):e03253. https://doi.org/10.1016/j.heliyon.2020.e03253

60. Afroze S, Sen TK, Ang HM (2016) Adsorption performance of continuous fixed bed column for the removal of methylene blue (MB) dye using Eucalyptus sheathiana bark biomass. Res Chem Intermed 42(3):2343–2364. https://doi.org/10.1007/s11164-015-2153-8

61. Aichour A, Zaghouane-Boudiaf H, Mohamed Zuki FB, Kheir-eddine Aroua M, Ibbora CV (2019) Low-cost, biodegradable and highly effective adsorbents for batch and column fixed bed adsorption processes of methylene blue. J Environ Chem Eng 7(5):103409. https://doi.org/10.1016/j.jece.2019.103409

62. Sheng L, Zhang Y, Tang F, Liu S (2018) Mesoporous/microporous silica materials: preparation from natural sands and highly efficient fixed-bed adsorption of methylene blue in wastewater. Microporous Mesoporous Mater 257:9–18. https://doi.org/10.1016/j.micromeso.2017.08.023

63. Boucherdoud A, Kherroub DE, Bestani B, Benderdouche N, Douinat O, History A (2022) Fixed-bed adsorption dynamics of methylene blue from aqueous solution using alginate-activated carbon composites adsorbents. Alger J Environ Sci Technol 8(1):2329–2337 https://www.aljest.net/index.php/aljest/article/view/551